

Open Research Online

The Open University's repository of research publications and other research outputs

Water line emission in low-mass protostars

Journal Item

How to cite:

Ceccarelli, C.; Caux, E.; Loinard, L.; Castets, A.; Tielens, A. G. G. M.; Molinari, S.; Liseau, R.; Saraceno, P.; Smith, H. and White, G. (1999). Water line emission in low-mass protostars. *Astronomy & Astrophysics*, 342(2) L21-L24.

For guidance on citations see [FAQs](#).

© 1999 European Southern Observatory (ESO)

Version: Version of Record

Link(s) to article on publisher's website:

<http://cdsads.u-strasbg.fr/abs/1999A%26A...342L..21C>

Copyright and Moral Rights for the articles on this site are retained by the individual authors and/or other copyright owners. For more information on Open Research Online's data [policy](#) on reuse of materials please consult the policies page.

oro.open.ac.uk

*Letter to the Editor***Water line emission in low-mass protostars***

C. Ceccarelli¹, E. Caux², L. Loinard³, A. Castets¹, A.G.G.M. Tielens⁴, S. Molinari⁵, R. Liseau⁶, P. Saraceno⁷, H. Smith⁸, and G. White⁹

¹ Laboratoire d'Astrophysique de l'Observatoire de Grenoble, B.P. 53X, F-38041 Grenoble Cedex, France

² CESR-CNES, 9 Avenue de Colonel Roche, F-31029 Toulouse, France

³ Institut de Radio Astronomie Millimétrique, 300 rue de la piscine, F-38406 St. Martin d'Hères, France

⁴ SRON, P.O. Box 800, 9700 AV, Groningen, The Netherlands

⁵ IPAC, California Institute of Technology, MS 100-22, Pasadena, CA 91125, USA

⁶ Stockholm Observatory, S-133 36 Saltsjobaden, Sweden

⁷ IFSI – CNR, Via del fosso del cavaliere 100, I-00133 Roma, Italy

⁸ Harvard-Smithsonian Center for Astrophysics, 60 Garden Street, Cambridge, MA 02138, USA

⁹ Queen Mary and Westfield College, Mile End Road, London E1 4NS, UK

Received 30 November 1998 / Accepted 7 January 1999

Abstract. Using the Long Wavelength Spectrometer aboard ISO, we have detected far infrared rotational H₂O emission lines in five low-mass young stellar objects in a survey of seven such sources. The total H₂O fluxes are well correlated with the 1.3 mm continuum fluxes, but – surprisingly – not with the SiO millimeter emission originating in the outflows, suggesting that the water emission arises in the circumstellar envelopes rather than in the outflows.

In two of the sources, NGC1333-IRAS4 and IRAS16293-2422, we measured about ten H₂O lines, and used their fluxes to put stringent constraints on the physical conditions (temperature, density and column density) of the emitting gas. Simple LVG modelling implies that the emission originates in a very small (~ 200 AU), dense ($\geq 10^7$ cm⁻³) and warm (~ 100 K) region, with a column density larger than about 10^{16} cm⁻². The detected H₂O emission may be well accounted for by thermal emission from a collapsing envelope, and we derive constraints on the accretion rate and central mass of NGC1333-IRAS4. We also discuss an alternative scenario in which the H₂O emission arises in an extremely dense shock very close to the central object, perhaps caused by the interaction of the outflow with the inner regions of the circumstellar envelope.

Key words: stars: formation – ISM: jets and outflows – ISM: individual objects: – infrared: ISM: lines and bands – radiative transfer – ISM: molecules

Send offprint requests to: C.Ceccarelli

* Based on observations with ISO, an ESA project with instruments funded by ESA Member States (especially the PI countries: France, Germany, the Netherlands and the United Kingdom) with the participation of ISAS and NASA.

1. Introduction

In the quiescent ISM, most water molecules are believed to be frozen into the icy mantles of the dust grains (e.g. van Dishoeck & Blake 1998). However, if a phenomenon energetic enough to evaporate or destroy those mantles occurs, water can be released into the gas phase. In addition, at temperature larger than about 250K, endothermic reactions in the gas phase can efficiently transform the oxygen not locked into CO molecules into H₂O molecules (Graff & Dalgarno 1987). Both effects can lead to high enhancements of the water gas phase abundance, and lead to intense emission in its far infrared rotational lines. Energetic phenomena and heating are known to occur near low-mass protostars: powerful outflows create strong shocks (e.g. Hollenbach & McKee 1989; Kaufman & Neufeld 1996), while in the infalling envelopes, heating due to the central source and/or to compression of the gas, may be sufficient to produce large over-abundances of water (Ceccarelli, Hollenbach & Tielens 1996). In this *Letter*, we report the detection of H₂O lines towards five sources from a sample of seven low-mass protostars.

2. Observations and results

The sample consists of seven young (Class 0 or I) sources, all of which located in the ρ Ophiuchus and NGC 1333 cloud complexes. While the distance to ρ Oph is fairly well known (120 pc – Knude & Hog 1998), the distance to NGC 1333 remains a matter of debate. The distance commonly used is 350 pc, but Cernis (1993) recently proposed a somewhat lower value of 200 pc. The latter value will be used here, but we emphasise that most of our conclusions would stand essentially unaffected if 350 pc was used instead.

The H₂O spectra were obtained using the *Long Wavelength Spectrometer* (hereafter LWS) on board the ISO satellite in the

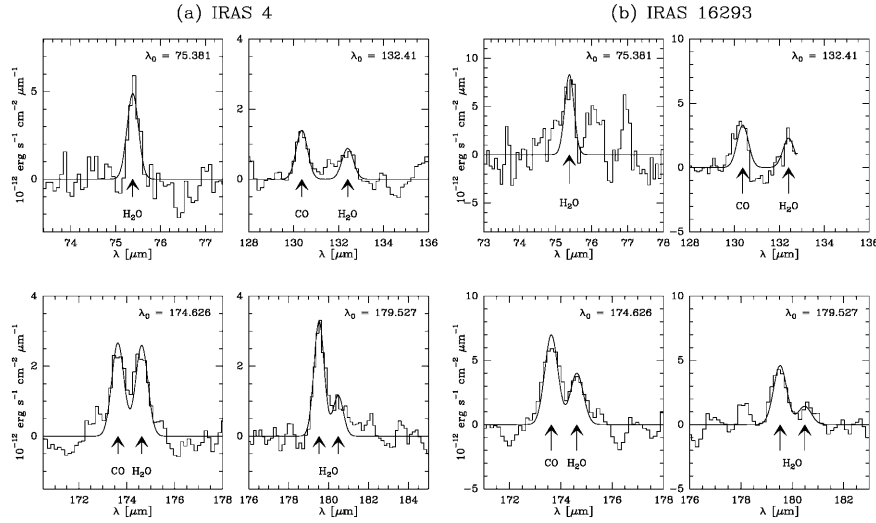


Fig. 1a and b. Selected H_2O lines towards IRAS4 (*left*) and IRAS16293 (*right*).

LWS01 mode. They cover the spectral range from 45 to 200 μm at a resolution of about 250; the beamwidth is $\sim 80''$. A more detailed description of the observations is given in Ceccarelli et al. (1998a) for IRAS16293-2422 (hereafter IRAS16293), Molinari et al. (in prep.) for SSV13, Ceccarelli et al. (in prep.) for EL29, and will be given in forthcoming papers for the other sources. We have also mapped the outflow powered by IRAS16293.

The LWS spectra consist of a continuum on which spectral features are superimposed. To obtain the fluxes of the water lines, the best first order polynomial fit to the continuum adjacent to the line was removed from the spectrum. The continuum is always at least 50 times stronger than the lines. The absolute flux calibration accuracy of LWS is better than 30% (Swinyard et al. 1996). In IRAS16293 the line blending was high and emission free baseline regions surrounding the H_2O lines were difficult to find (see Ceccarelli et al. 1998b). As a consequence, although the H_2O lines in IRAS16293 are usually brighter than those in IRAS4, less lines could be safely identified (and their fluxes measured).

The fluxes of about 8 and 12 H_2O lines could be measured towards IRAS16293 and IRAS4 respectively (Fig. 1), while only a few lines were detectable towards three other sources (Table 1¹), and no emission could be detected towards IRAS16293-SE² and NGC1333-IRAS6 at a detection limit of $\sim 7 \times 10^{-13}$ $\text{erg s}^{-1}\text{cm}^{-2}$. Finally, H_2O emission was not detected along the outflow powered by IRAS16293, not even at the positions where the SiO and low J CO lines are the strongest, with upper limits on the 179 μm line (usually the brightest H_2O line) $\leq 1/3$ that of the IR source.

3. Discussion

3.1. Correlations

The water lines detected towards the sources of our sample could *a priori* emanate from shocks (associated or not with their out-

Table 1. Water line fluxes (in $10^{-12}\text{erg s}^{-1}\text{cm}^{-2}$) detected towards the sources of the sample. The statistical errors are ~ 0.2 or less in these units.

λ (μm)	Trans.	ρ Oph 16293	1333 IRAS4	1333 IRAS2	1333 SSV13	ρ Oph EL 29
180.5	$2_{21} - 2_{12}$	0.9	0.7	≤ 0.3	0.4	
179.5	$2_{12} - 1_{10}$	2.9	2.1	0.6	0.5	≤ 1.5
174.6	$3_{03} - 2_{12}$	2.5	1.7	≤ 0.5	1.1	0.9
138.5	$3_{13} - 2_{02}$	0.9	0.9			
132.4	$4_{23} - 4_{14}$	1.3	0.6	0.3	≤ 0.3	≤ 0.6
108.1	$2_{21} - 1_{10}$		1.7	0.4		
101.0	$3_{03} - 2_{20}$	1.3	1.1			
90.0	$3_{22} - 2_{11}$	0.5	1.8			
99.5	$5_{04} - 4_{14}$		1.0			
78.7	$4_{23} - 3_{12}$		0.9			
75.4	$3_{21} - 2_{12}$	2.7	1.7	≤ 1	≤ 1	
67.3	$3_{30} - 3_{03}$		0.6			

flows), or from the innermost and warmest regions of their central envelopes and/or disks. To try to clarify their origin, we compare the fluxes of the water lines with quantities related to each mentioned component. The total water line flux will be estimated by the sum of the fluxes in the 180, 179, 174 and 132 μm lines. Those lines were chosen first because they cover a wide range of upper level energies and are therefore a good measure of the total H_2O line flux for a wide range of density and temperature values; and second because they are the strongest lines, and could be measured in several objects.

As a parameter able to “measure” the shocks we chose the SiO emission, integrated all over the velocities³, observed towards each source, smoothed to the 80'' resolution of ISO-LWS, using the complete SiO maps of the NGC1333 region obtained by Castets et al. 1998 and of the region surrounding IRAS16293

³ The narrow component observed in some of these sources (Lefloch et al. 1998) and associated with the cloud rather than with the source does not contribute significantly to the reported emission in any of these sources.

¹ SSV13 is sometime reported in literature as SVS13.

² 16293-SE is a recently discovered young source (Loinard et al., in prep.).

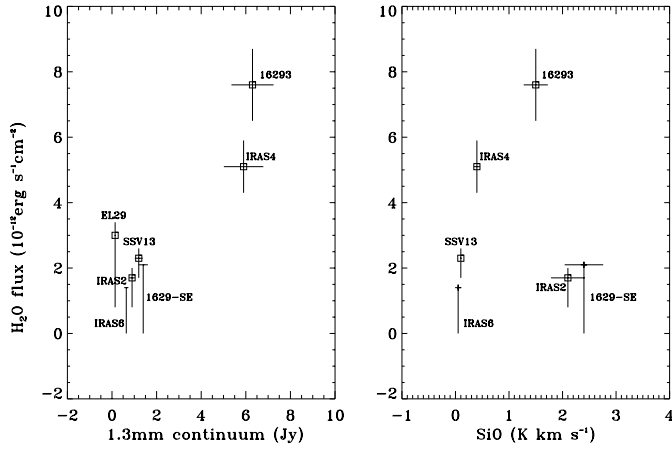


Fig. 2. H₂O emission as a function of SiO emission (*right*) and 1.3 mm emission (*left*). The error bars of the H₂O, SiO and 1.3mm fluxes represent the error on the calibration only and were taken to be 30%.

by Castets et al. (in prep.). There is *no correlation* between the SiO and the H₂O fluxes (Fig. 2 right). Since SiO emission is believed to be indicative of strong shocks ($\geq 50 \text{ km s}^{-1}$, see e.g. Flower & Pineau de Forets 1995), this lack of correlation implies either that *water forms in lower velocity shocks (which however do not occur where the high velocity shocks are found)* or that *water does not originate in shocks*. The lack of SiO-H₂O emission correlation is further strengthened by the non-detection of H₂O towards the outflow powered by IRAS16293, where SiO emission is very strong.

On the other hand, there seems to be a correlation between the H₂O flux and the 1.3 mm continuum emission (taken from Saraceno et al. 1996), in the sense that sources having higher millimeter fluxes have higher H₂O luminosities (Fig. 2 left). Since the 1.3 mm continuum flux traces the envelopes surrounding such young sources (e.g. Saraceno et al. 1996) rather than the disks (Butner et al. 1990), this correlation may imply either that *water emission is associated to the thermal emission from the envelopes themselves*, or that *it originates in shocks where the shocked material belongs to the envelopes*.

3.2. Physical conditions of the emitting gas

The ratio between the H₂O line fluxes in IRAS16293 and IRAS4 are fairly similar in all the detected lines (Table 1), implying that the physical conditions in both sources (i.e. gas temperature and density) are similar as well. For the other sources, the small number of transitions detected does not significantly constraint the parameter space.

To constraint the physical conditions of the emitting gas, we modelled the H₂O lines using an LVG code. This model takes into account the first 48 rotational levels of ortho H₂O (the collisional excitation rates are from Green et al. 1993), but does not take into account the continuum emission. The spectroscopic data are taken from the JPL catalogue (Pointer & Pickett 1985). LVG predictions depend upon four parameters: the density and the temperature of the gas, the angular extent of the emitting region and the H₂O column density divided

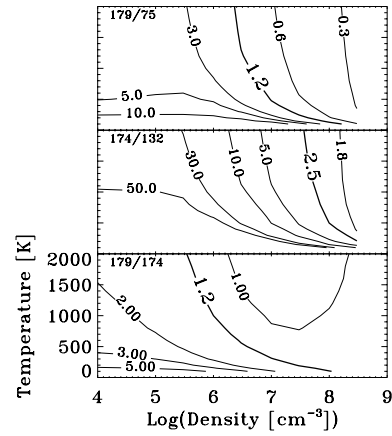


Fig. 3. Ratios between the 179 and 174 μm lines (*bottom*), 174 and 132 μm lines (*middle*) and 179 and 75 μm lines (*top*). The observed values are shown by the thick lines.

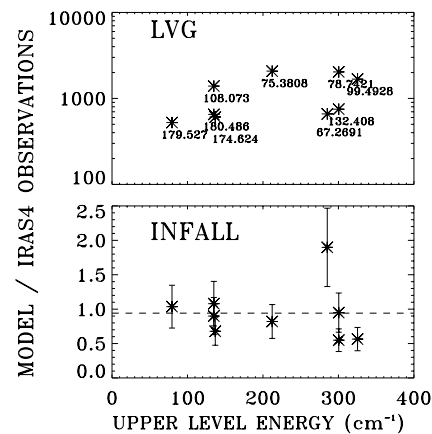


Fig. 4. Ratio between LVG model (*top*) or “infalling envelope” model (*bottom*) and observations of IRAS4.

by the velocity gradient (which regulates the optical depth of the lines). The line ratios on the other hand depend mainly on the gas temperature and density, and to a smaller extent on the column density when the lines are optically thick. Hence, in the first step, we used the observed line ratios to estimate the temperature, density and H₂O column density of the gas, and later compared the absolute fluxes deduced from the model with the observed fluxes to infer the angular extent of the source.

The models were applied to IRAS16293 and to IRAS4, and used the ratios between the 179, 174, 132 and 75 μm lines (which cover the widest range of upper level energies). Comparison between the model predictions and the observed line ratios (Fig. 3) shows that the emitting gas is dense ($n \geq 10^7 \text{ cm}^{-3}$) and warm ($T \sim 100 \text{ K}$) and that the lines are optically thick. In particular, the lines at 132 μm and 75 μm set stringent constraints on the density *and* H₂O column density which has to be larger than 10^{16} cm^{-2} (the two quantities are not totally independent from each other). One of the best fit to the IRAS4 data is obtained for $n = 2 \times 10^8 \text{ cm}^{-3}$, $T = 200 \text{ K}$, and $N(\text{H}_2\text{O}) = 10^{16} \text{ cm}^{-2}$ (where we used a linewidth equivalent to $\Delta v = 10 \text{ km s}^{-1}$). The ratio between the predictions of this model and the observed values

(top of Fig. 4) implies a beam filling factor of about $1/800 \times \frac{\Delta v}{10 \text{ km s}^{-1}}$. The corresponding angular size of the emitting region is therefore $\sim 2\text{--}3''$, corresponding to a physical size of a few hundred AU. Slight discrepancies between the model and the observations occur systematically for the shorter wavelength lines, and may be a consequence of the lack of continuum background in our computations.

Finally, we note that the ratio between the 179 and the 174 μm lines is five times greater in HH54B than in all our sources. This indicates that the emitting regions are either much denser or much warmer (or both) in our sources than in HH54B, where the emission was ascribed to a mild shock (Liseau et al. 1996). In conclusion, the analysis of this paragraph and of the previous one lead to a rather clear situation and two possibilities to explain the observed H_2O emission: a) it is emitted in a very dense, warm and compact region, excited by a dense and relatively slow shock close to the central object, may be caused by the interaction of the outflow with the inner regions of the circumstellar envelope, or b) to the thermal emission of these regions. We will consider in more detail these two possibilities in the next two paragraphs.

3.3. The dense shock hypothesis

As noted above, if the H_2O emission has to be attributed to a shock this is a shock totally different to those responsible for the SiO emission, implying a rather low velocity ($\leq 50 \text{ km s}^{-1}$). The presence of such a shock very close to the central object and due to the interaction of the outflow with the dense environment is suggested by the strong 22 GHz H_2O maser emission ($\sim 10^{-9} L_\odot$) with velocities ($\geq 7 \text{ km s}^{-1}$) in excess of the relevant keplerian velocities (e.g. Claussen et al 1996). The best-fit LVG model mentioned in the previous paragraph predicts a 22 GHz luminosity $\sim 4 \times 10^{-11} L_\odot$, much lower than the mentioned observations. Moreover the masers in the IRAS4 and IRAS16293 differ by orders of magnitudes, whereas the H_2O FIR emission is very similar. This may suggest that the FIR emission is *not* related to the 22 GHz emission arising from the outflow.

3.4. The infalling envelope model

The second possibility is that the observed H_2O lines originate from the warm inner region of the envelope. In order to test this hypothesis we used the model of an infalling envelope developed by Ceccarelli, Hollenbach & Tielens (1996), which self consistently computes the chemical composition, thermal balance and emerging far infrared line spectrum within the framework of the “inside-out” collapse (Shu 1977). The H_2O line fluxes observed towards IRAS4 can be well reproduced by this model for a central source mass of $\sim 0.3 M_\odot$ and a mass accretion rate of $\sim 3 \times 10^{-5} M_\odot \text{ yr}^{-1}$ (bottom of Fig. 4). In this model, the H_2O emission originates ≤ 150 AU from the central source, where the density is $\geq 5 \times 10^7 \text{ cm}^{-3}$, and the temperature high enough to evaporate the icy dust grain mantles. This infall model also predicts that the 22 GHz H_2O line should maser at a distance ~ 80 AU from the central source, have a luminosity $\sim 3 \times 10^{-10}$

L_\odot , and a velocity close to the systemic velocity. Most of the components towards IRAS4 reported by Claussen et al. (1996) have velocities which differ from that of the source, and are likely to be associated to the outflow. However, one component at about the velocity of the source was detected (bottom of their Fig. 3) with an intensity in good agreement with the predictions of this model.

4. Conclusions

Water line emission was detected towards 5 of the 7 sources in our sample. In IRAS4 and IRAS16293, the fluxes of about ten lines could be measured; they show that the physical conditions (temperature and density) of the emitting regions are fairly similar in both sources. The H_2O emission flux does not correlate with the SiO emission associated with their outflows, but seems to be related to the 1.3 mm continuum flux of the sources. This suggests that the emission originates in the circumstellar envelopes rather than in the outflows. Simple LVG modeling of the line intensities shows that the H_2O emission originates in a compact ($\sim 2''$), dense ($n \geq 10^7 \text{ cm}^{-3}$) and warm ($T \sim 100 \text{ K}$) gas, with H_2O column densities $\sim 10^{16} \text{ cm}^{-2}$. Finally, the water lines observed towards IRAS4 can be successfully modeled within the framework of an infalling envelope (Ceccarelli et al. 1996), if the central source mass is $\sim 0.3 M_\odot$ and the mass accretion rate $\sim 3 \times 10^{-5} M_\odot \text{ yr}^{-1}$. However, we cannot exclude that some of the observed H_2O emission originates in a shock very close to the central object, the same responsible for most of the 22 GHz maser emission seen towards our sources.

Acknowledgements. We are grateful to A. Wootten for invaluable informations on the water masers associated to IRAS4 and IRAS16293, and to J. Knude for his informations on the distances to NGC 1333 and ρ Oph. We also thank F.Motte and P.André for providing us their millimeter data of the IRAS16293 region prior to publication and W.Pfau, the referee, for carefully reading the manuscript. Finally, we acknowledge the dedication of the LWS team which made these observations possible.

References

- Butner A., Evans N.J.II, Lester D.F., Levreault R., Strom S.E. 1991, ApJ 373, 636
- Ceccarelli C., Hollenbach D.J., Tielens A.G.G.M. 1996, ApJ 471, 400
- Ceccarelli C., Caux E., White G. et al. 1998a, A&A 331, 372
- Ceccarelli C., Caux E., Wolfire M. et al. 1998b, A&A 331, L17
- Claussen M.J., Wilking B.A., Benson P.J. et al. 1996, ApJS 106, 111
- Cernis K. 1993, Baltic Astronomy 2, 214
- Graff M.M., Dalgarno A. 1987, ApJ 317, 432
- Green S., Malauendes S., McLean A.D. 1993, ApJS 85, 181
- Hollenbach D.J., McKee C.F. 1989, ApJ 342, 306
- Kaufman M.J., Neufeld D.A., 1996, ApJ 456, 611
- Knude J., Hog E. 1998, A&A 338, 897
- Lefloch B., Castets A., Cernicharo J., Loinard L. 1998, ApJ 504, L109
- Liseau R., Ceccarelli C., Larsson B., et al. 1996, A&A 315, L181
- Flower D.R. & Pineau de Forets 1995, MNRAS 275, 1049
- Pointer R.L. & Pickett H.M. 1985, Applied Optics 24, 2235
- Saraceno P., André P., Ceccarelli C. et al. 1996, A&A 309, 827
- Shu F.H. 1977, ApJ 214, 488
- Swinyard B.M., Clegg P.E., Ade P.A.R. et al. 1996, A&A 315, L43
- van Dishoeck E. & Blake, G.A. 1998, Ann.Rev.Astr.Ap. 317